Biology Direct

RESEARCH

Open Access

Enhanced itaconic acid secretion from macrophages mediates the protection of mesenchymal stem cell-derived exosomes on lipopolysaccharide-induced acute lung injury mice

Yanmei Wen[1,2] and Zong'an Liang[1*]

Abstract

Background Alveolar macrophages (AMs) is critical to exacerbate acute lung injury (ALI) induced by lipopolysaccharide (LPS) via inhibiting inflammation, which could by shifted by mesenchymal stem cell-derived exosomes (MSC-exos). But the underlying rationale is not fully clarified. Our study aimed to analyze the significance of itaconic acid (ITA) in mediating the protective effects of MSC-exos on LPS-induced ALI.

Methods MSC-exos were used to treat pulmonary microvascular endothelial cells (PMVECs) co-cultured with AMs under LPS stimulation. si-IRG1 was transfected to AMs. PMVEC permeability, apoptosis rates, and inflammatory cytokine levels were assessed. In vivo, C57BL/6 wild-type (WT) and Irg1−/− mice were employed to explore the protection of MSC-exos against LPS-induced ALI. The lung injury was determined by histological and biochemical assays. ITA levels were measured using gas chromatography-mass spectrometry. Western blot and flow cytometry analyses were performed to assess M1/M2 polarization.

Results Co-culture with AMs significantly increased PMVEC permeability, apoptosis rates, IL-6, TNF-α levels and Claudin-5 and ZO-1 expression induced by LPS treatment, which were attenuated by MSC-exos accompanied by enhanced ITA level. After si-IRG1 transfection, MSC-exos' protective efficacy was reversed, with suppressed M2 polarization. In vivo, MSC-exos alleviated alveolar structure disruption, pulmonary edema, inflammation and increased ITA concentration in WT mice but had reduced effects in Irg1−/− mice, with neglected M2 polarization.

Conclusions ITA secretion facilitated the MSC-exos' protective benefits on LPS-induced PMVEC damage and ALI in mice by promoting AM M2 polarization, highlighting a potential therapeutic strategy for ALI and related inflammatory lung diseases.

Keywords Acute lung injury, Mesenchymal stem cell-derived exosomes, Itaconic acid, Alveolar macrophages, Inflammation

*Correspondence:
Zong'an Liang
liangza@scu.edu.cn

[1]Department of Respiratory and Critical Care Medicine, West China Hospital, Sichuan University, No. 37, Guoxue Lane, Wuhou District, Chengdu 610000, Sichuan, China
[2]Department of Respiratory and Critical Care Medicine, Chengdu Second People's Hospital, Chengdu 610000, Sichuan, China

Background

Acute lung injury (ALI) features severe damage to the alveolar epithelium and vascular endothelium. This condition can lead to increased pulmonary permeability, pulmonary edema, and potentially acute respiratory distress syndrome, which links to a high fatality rate [1]. In addition, survivors may experience long-term declines in lung function and significant reductions in quality of life [1]. Therefore, it is crucial to explore novel therapeutic strategies and improve the prognosis of ALI patients. The forefront of research in ALI includes numerous emerging therapeutic strategies. For instance, gene therapy and RNA interference techniques have shown promise in protecting lung tissue by inhibiting specific inflammatory genes to reducing the inflammatory response [2, 3]. Immune checkpoint inhibitors and antibody therapies aim to mitigate ALI symptoms by modulating the immune system and neutralizing inflammatory mediators [4]. Notably, mesenchymal stem cell-derived exosome (MSC-exos) has garnered widespread attention in recent years.

MSC-exos contain various bioactive molecules to regulate the functions of recipient cells and facilitate intercellular communication [5]. In co-culture models of lung organoids and macrophages, MSC-exos showed the ability to reduce the secretion of pro-inflammatory cytokines and promote lung tissue repair via the NF-κB pathway [6]. In murine models, adipose tissue-derived MSC-exos ameliorated ALI by restoring mitochondrial integrity in alveolar macrophages (AMs), facilitating their transformation into an anti-inflammatory phenotype and improving immune homeostasis [7]. Macrophages, particularly AMs, play a critical role in these processes. They regulate the inflammatory response through M1 pro-inflammatory and M2 anti-inflammatory polarization shifts [8]. Moreover, macrophages can modulate ALI through immune regulation and metabolic reprogramming [9]. The regulatory mechanisms of macrophages in ALI are highly complex and although MSC-exos are proven to be able to alleviate ALI by regulating macrophages [8], the specific mechanisms underlying this regulation represent a significant area for further exploration.

Itaconic acid (ITA) is a critical metabolic product catalyzed by the enzyme IRG1 in macrophages [10]. It achieves its anti-inflammatory effects by blocking succinate dehydrogenase, thereby decreasing reactive oxygen species. It also modulated the balance of pro- and anti-inflammatory cytokines like IL-1β and IL-10, respectively [11, 12]. This anti-inflammatory property has been demonstrated to improve inflammation-related disease. For instance, itaconate derivative had the ability to modulate the fatty liver disease in male mice [13]. However, the exact mechanisms by which ITA conducts regulatory function in the improvement of ALI by MSC-exos remain unclear.

Therefore, our study investigated the character of ITA in mediating the protective effects of MSC-exos and indicated that MSC-exos significantly alleviate lipopolysaccharide (LPS)-induced PMVEC injury and ALI by enhancing ITA secretion and promoting AM M2 polarization. These findings suggest a potential therapeutic strategy for lung diseases associated to inflammation.

Methods

Ethic statement

All animal experiments were conducted aligned with the guidelines of Institutional Animal Care and Use Committee. Prior to the initiation of the study, approval was obtained from the ethics commitee of Sichuan University. Mice were maintained under 22±2 °C, 50±10% humidity in 12-hour light/dark cycle, with *ad libitum* access to food and water.

Animal experiment schedule

Male C57BL/6 wild-type (WT) mice and Irg1 knockout (Irg1−/−) mice (C57BL/6NJ-Acod1em1(IMPC)J/J, stock #029340) aged 8–10 weeks were purchased from the Jackson Laboratory (Bar Harbor, ME, USA). Mice were subjected to 10 mg/kg LPS treatment via intratracheal injection to induce ALI. The LPS solution was administered into the trachea using a micro-sprayer aerosolizer. Ten hours post-LPS administration, 50 μg of MSC-exos or PBS was administered intratracheally. Mice were euthanized by overdose inhalation of isoflurane 24 h after LPS injury. Both WT and Irg1−/− mice were divided into three groups (n=12 per group): Sham group: received intratracheal PBS without LPS; LPS group: received 10 mg/kg LPS without MSC-exos; and LPS+MSC-exos group: received 10 mg/kg LPS followed by 50 μg MSC-exos. After euthanasia, lung tissues and bronchoalveolar lavage fluid (BALF) were collected and prepared for biochemical and histological parameter determination.

Cell culture and treatment

Mouse pulmonary microvascular endothelial cells (PMVECs; CP-M001) were purchased from Procell Life Science (Wuhan, China) and maintained in endothelial cell growth medium (Procell) supplemented with 10% fetal bovine serum (FBS) and 1% penicillin-streptomycin (p/s). Mouse alveolar macrophages (Ams; iCell-m078; iCell Bioscience, Shanghai, China) MH-S cell line was cultured in RPMI-1640 medium (Gibco, Waltham, MA, USA) supplemented with 10% FBS and 1% p/s. Both were maintained at 37 °C in a humidified atmosphere containing 5% CO_2.

To evaluate the impact of AMs on PMVECs, PMVECs were seeded at a density of 1×10^5 cells per well in 24-well

plates at the presence of AMs seeded at a same density in the upper chamber of a Transwell insert (0.4 μm pore size, Corning, Corning, NY, USA) or alone. Co-cultured or alone-cultured cells were subsequently treated with LPS at a dose of 100 ng/mL for 24 h. To investigate the effect of MSC-exos on LPS-induced PMVEC injury and AM polarization, 50 μg/mL MSC-exos were added into co-culture system for 24 h. And to evaluate whether ITA mediates the protective effects of MSC-exos, MH-S cells were transfected with siRNAs targeting IRG1. Post-transfection, the LPS-stilulated cells were treated with MSC-exos (50 μg/mL) for 24 h. After incubation, PMVECs, MH-S cell pellets or supernatant were collected for further assays.

Isolation and characterization of exosomes from MSCs

MSCs were purchased from Gibco and characterized via staining of surface markers and accessing adipogenic, osteogenic, and chondrogenic differentiation potential (Figure S1A-G). Cells were cultured in Dulbecco's Modified Eagle Medium (DMEM; Gibco) supplemented with 10% FBS without exogenous exosomes and 1% p/s. When MSCs reached approximately 80% confluence, the culture medium was replaced with exosome-depleted FBS medium, and cells were cultured for an additional 48 h. The conditioned medium was then collected and conducted a series of centrifugation. The resulting supernatant was subjected to ultracentrifugation at 100, 000 × g for 70 min at 4 °C. The pellet containing exosomes was washed by ultracentrifugation and resuspended in 100 μL of PBS. The morphology of MSC-exos were characterized by transmission electron microscopy (TEM; JEM-1230, JEOL Ltd., Tokyo, Japan; Figure S1H). The size distribution of the isolated exos was determined using nanoparticle tracking analysis (NTA) with a NanoSight NS300 system (Malvern Instruments, Malvern, UK). Western blot analysis was performed to confirm the presence of exosomal markers including CD63, TSG101 and Calnexin as a negative control (Figure S1J).

Cell transfection

MH-S AMs were transfected with three types of siRNAs targeting IRG1 and a non-targeting control siRNA (si-NC) using an optimized electroporation method as previously described [14]. Before transfection, cells were transferred to fresh RPMI medium and cultured for 24 h. For differentiation, 1.5×10^7 cells were seeded in 75 cm^2 flasks with RPMI-1640 medium containing 10% FCS, 1% PSG, 1% sodium pyruvate, 1% non-essential amino acids, 10 ng/ml PMA, and 50 μM β-mercaptoethanol, and cultured for 48 h. For nucleofection, cells were detached using Accutase I, centrifuged, and resuspended in prewarmed RPMI medium at a density of 2.5×10^6 cells were prepared per transfection. Subsequently, siRNA was diluted in nuclease-free water, and 1 μg siRNA was mixed with cells in Nucleofector solution. Cells were transfected using a Nucleofector 2b device and program Y-001.

Polymerase chain reaction (PCR)

The transfection efficiency of siRNAs into AMs were determined using the PrimeScript RT-PCR Kit (Takara, Kusatsu, Japan). TRIzol (Invitrogen, Carlsbad, USA) was used to extract the total RNA of cells. The cDNA was synthesized by The Reverse Transcription Kits (ThermoFisher, Carlsbad, USA) according to the instructions recommended by manufacturer. The Mini PCR Thermal Cycler (Sigma-Aldrich, Shanghai, China) was used to conduct thermal cycling as followes: begining at 95 °C for 5 min and continued for 40 cycles, consisting of 95 °C for 30 s, followed by 59 °C for 30 s, and 72 °C for 30 s in each cycle. The primer sequences are listed in Table S1. The relative expression levels of target genes were calculated using the $2^{-\Delta\Delta Ct}$ method with GAPDH as the internal control.

HRP permeability assay

PMVEC permeability was assessed using the SignalUp™ Super Sensitive ELISA Assay Kit with Fluorescent HRP Substrate (P0205S; Beyotime, Beijing, China). After the treatment period of cells, the medium in the upper chamber was replaced with 0.5 mL of fluorescein isothiocyanate (FITC)-conjugated dextran solution at a concentration of 1 mg/mL and the lower chamber contained PBS. The plates were incubated at 37 °C in a humidified atmosphere of 5% CO_2 for 2 h. The medium from the lower chamber was then collected, and the fluorescence intensity was measured using a microplate reader (BioTek Instruments Inc., Winooski, VT, USA) at an excitation wavelength of 490 nm and an emission wavelength of 520 nm. The permeability was calculated based on the fluorescence intensity, following the manufacturer's instructions provided with the protocol provided by the manufacturer.

Flow cytometry

Apoptosis of PMVECs was assessed using the Annexin V-FITC/PI Apoptosis Detection Kit (Beyotime) according to manufacturer's protocols. Following treatment, PMVECs were harvested by trypsinization, washed twice, and resuspended in 1× binding buffer at a concentration of 1×10^6 cells/mL. Subsequently, 100 μL of the cell suspension was incubated with 5 μL of Annexin V-FITC and 5 μL of PI for 15 min at room temperature in the dark.

To assess M2 polarization [15], treated AMs or mouse lung cell were prepared as suspension. For surface staining, 1×10^6 cells were incubated with anti-mouse CD206-PE antibody (BioLegend, San Diego, CA, USA) at a dilution of 1:100 for 30 min at 4 °C in the dark. Following

incubation, cells were washed twice with staining buffer and resuspended in staining buffer.

The samples were analyzed using BD FACSCanto II flow cytometer (BD Biosciences, San Jose, CA, USA). Data were acquired and analyzed using FlowJo software (Version 10.7, FlowJo LLC, Ashland, OR, USA).

TUNEL assays

After treatment, cells were fixed with a 4% paraformaldehyde solution and were then permeabilized with 0.1% TritonX-100 for 2 min. Following this, the cells were washed with PBS and stained with TUNEL reagent from the Cell Death Detection Kit (Roche, Mannheim, Germany). Subsequently, they were stained with DAPI at a concentration of 0.1 μg/ml for 5 min. The images were captured at 40× magnification using an Olympus DP 74 fluorescence microscope (Tokyo, Japan).

Determination of inflammatory cytokines

The levels of IL-6 and TNF-α in the supernatant of cultured cells or BALF of mice were assessed by Mouse IL-6 and TNF-α ELISA kit (SEKM-0007 and SEKM-0034; Solarbio, Beijing, China), respectively. Briefly, 96-well microplates were coated with antibodies provided by kits and incubated overnight at 4 °C. The plates were washed, blocked, followed by prepared supernatant or standard cytokine solution incubation. Subsequently, the washed plates were added with biotinylated detection antibodies and streptavidin-conjugated HRP. The plates were developed with TMB substrate and the absorbance was measured after 20 min at 450 nm.

Gas chromatography-mass spectrometry (GC-MS) detection of ITA concentration

For GC-MS analysis, 200 μL of cell supernatant or plasma of mice was mixed with 50 μL of 2 mg/mL succinic acid and 50 μL of 0.5 M hydrochloric acid to acidify the sample. The mixture was then extracted with 1 mL of ethyl acetate by vigorous shaking for 10 min. The organic phase was collected, and the extraction was repeated twice. Combined organic phases were evaporated to dryness and the dried residue was reconstituted in 100 μL of ethyl acetate and derivatized with 100 μL of N, O-bis trifluoroacetamide with 1% trimethylchlorosilane at 60 °C for 30 min. Derivatized samples were analyzed using an Agilent 7890 A GC system coupled with an Agilent 5975 C mass selective detector (Agilent Technologies, Santa Clara, CA, USA). Data acquisition and analysis were performed using Agilent MassHunter software (Version B.07.00, Agilent Technologies).

Hematoxylin–eosin (H&E) staining

The lung tissues collected from mice were fixed with 4% paraformaldehyde for 48 h. After fixation, dehydrated through a graded series of ethanol, cleared in xylene, and embedded in paraffin. Serial sections were cut in 5 μm thickness from paraffin blocks, which were subsequently deparaffinized and rehydrated to distilled water. The sections were stained with H&E trichrome solutions (Sigma-Aldrich). Images were captured with a light microscope (Nikon Eclipse E200, Nikon, Melville, NY, USA).

Evaluation of mouse pulmonary edema

The lung wet/dry weight ratio was determined to assess pulmonary edema. The collected lungs were immediately weighed to obtain the wet weight using an analytical balance. Following that, the lungs were placed in a preweighed aluminum dish and dried in an oven at 60 °C for 72 h. After drying, the lungs were weighed to obtain the dry weight. The ratio provides an index of lung water content, with higher values indicating increased pulmonary edema.

Biochemical parameters in BALF

The total protein concentration in BALF was measured using the Pierce BCA Protein Assay Kit (Thermo Fisher Scientific, Waltham, MA, USA) according to the manufacturer's instructions. Briefly, 25 μL of BALF supernatant was mixed with 200 μL of BCA working reagent prior to being incubated at 37 °C for 30 min, and the absorbance was measured at 562 nm. Protein concentration was calculated from a standard curve. For neutrophils cell counting, cytospin preparations were made by centrifuging 100 μL of the cell suspension onto glass slides at 300 g for 5 min. The slides were then stained with Diff-Quik staining kit (Siemens, Newark, DE, USA). Neutrophils were identified and counted based using a light microscope at 400× magnification. A minimum of 200 cells per slide were counted.

Lung injury scoring

The degree of lung injury was evaluated based on a scoring system that included alveolar edema, hemorrhage, alveolar septal thickening, and infiltration of polymorphonuclear leukocytes. Each parameter was scored on a scale from 0 (normal degree with no visible damage) to 3 (severe degree with extensive damage). And score 1 and 2 represented a mild degree with minimal damage and a moderate degree with moderate damage, respectively. The total lung injury score was calculated by summing the scores of the four parameters. Lung injury was evaluated in a blinded manner by two independent pathologists to ensure accuracy and consistency.

Western Blot

The proteins of treated cells or lung cells prepared from mice were extracted by RIPA buffer (Abcam, Shanghai, China). Their protein concentrations were then

quantified using QuantiPro BCA Assay Kit (Sigma-Aldrich, St. Louis, MO, USA). Prepared samples were separated by SDS-polyacrylamide gel electrophoresis before transferred to nitrocellulose membrane, which was subsequently probed against zonula occluden (ZO)-1, Claudin-5, iNOS, Arg-1, IRG1, and GAPDH as primary antibodies followed by incubated with horseradish peroxidase-labeled secondary antibodies (Table S2). All primary and the secondary antibody were used in dilution of 1: 500 or 1: 2000, respectively. Bands were processed with enhanced chemiluminescence prior to being analyzed via the ChemiDoc imaging system (Bio-Rad, Hercules, CA, USA). Relative expression levels of target proteins were finally calculated using ImageLab software (Bio-Rad).

Statistical analysis

Statistical analyses were performed using GraphPad Prism software (version 8.0; GraphPad Software, San Diego, CA, USA). All data were presented as mean ± standard error of the mean (SEM). For comparisons among groups, one-way analysis of variance (ANOVA) followed by Tukey's post hoc test were conducted for normally distributed data, whereas Kruskal-Wallis test followed by Dunn's post hoc test were used for non-normally distributed data. A P-value < 0.05 was considered statistically significant.

Results

AMs aggravate LPS-induced injury in PMVECs via M1 polarization-mediated inflammatory response

PMVECs were cultured in the presence of AMs or alone, with 100 ng/mL LPS treatment. Equivalent PBS was used as the control, as shown in Fig. 1A. After 24-h culture, PMVEC permeability was assessed using HRP leakage assays. The permeability was increased in the PMVECs + LPS and PMVECs + AMs + LPS compared to their counterparts without LPS simulation. The highest HRP permeablity was found in the PMVECs + AMs + LPS group, indicating that co-culture with AMs significantly exacerbated the endothelial barrier disruption under LPS treatment (Fig. 1B). Western blot analysis revealed that LPS treatment suppressed the relative expressions of Claudin-5 and ZO-1 proteins [16], with the lowest levels in the AMs co-culture group (Fig. 1C). The flow cytometry and TUNEL assays demonstrated that LPS treatment increases the apoptosis rate of PMVECs (Fig. 1D and E). In the presence of AMs, LPS-treated PMVECs showed higher levels of apoptosis compared the those cultured alone. ELISA assays for inflammatory cytokines IL-6 and TNF-α demonstrated that their levels were enhanced with LPS treatment, and further increased with AMs co-culture (Fig. 1F and G). Additionally, the western blot analysis for M1 polarization marker iNOS and Arg-1 showed a lower expression in PMVECs + AMs group compared to the IFN-γ/LPS control. Both of these proteins were increased in the PMVECs + AMs + LPS group compared to the co-cultured cells without LPS treatment (Fig. 1H). It suggested that LPS stimulation in the presence of AMs induces a stronger M1 polarization, which contributes to the inflammatory response, in PMVECs.

MSC-exos attenuate LPS-induced PMVEC injury by promoting M2 polarization of AMs

The characteristics of MSCs and their derived exosomes was confirmed initially. The high levels of positive markers CD44 and CD90 (> 95%; Figures S1A and B) and low levels of hematopoietic markers CD31 and CD45 (< 5%; Figures S1C and D) expressed in cells indicated their mesenchymal origin. Differentiation potential was demonstrated by osteogenesis (Figure S1E), adipogenesis (Figure S1F) and chondrogenesis (Figure S1G). TEM revealed the characteristic cup-shaped morphology of exosomes (Figure S1H) and NTA verified a size distribution consistent with exosomes, with a peak around 70–75 nm (Figure S1I). Western blot analysis further confirmed the exosome markers TSG101 and CD63, with the absence of the endoplasmic reticulum marker Calnexin indicating the purity of the exosome preparation (Figure S1J). After confirmation of the successful generation of MSC-exos, they were added to the LPS-treated co-culture system to evaluate the effects of MSC-exos on PMVECs. PMVEC permeability was assessed using HRP leakage assays, which showed that the significantly increased permeability in the PMVECs + AMs + LPS group was attenuated by the addition of MSC-exos (Fig. 2A). Western blot analysis suggested that the expression of both Claudin-5 and ZO-1 were significantly decreased in the LPS group, but was restored upon MSC-exos administration (Fig. 2B). Additionally, both Annexin V-FITC/PI staining (Fig. 2C) and TUNEL assays (Fig. 2D) demonstrated that the increased apoptosis rate of PMVECs induced by LPS was inhibited by MSC-exos. ELISA assays for inflammatory cytokines IL-6 and TNF-α illustrated that despite their levels being increased with LPS treatment, the addition of MSC-exos significantly reduced the levels of both cytokines (Fig. 2E and F). Western blot analysis for M1 polarization markers revealed that the expression of iNOS and Arg-1 proteins were increased in the PMVECs + AMs + LPS group and were significantly reduced by MSC-exos treatment (Fig. 2G). Then, the M2 polarization was determined by the percentage of CD206-positive cells, which increased from approximately 5% in the control group to 8% with LPS treatment, and further to 15% with MSC-exos treatment (Fig. 2H). Finally, GC-MS was used to measure ITA concentration, which increased by LPS treatment and was further significantly increased by MSC-exos (Fig. 2I).

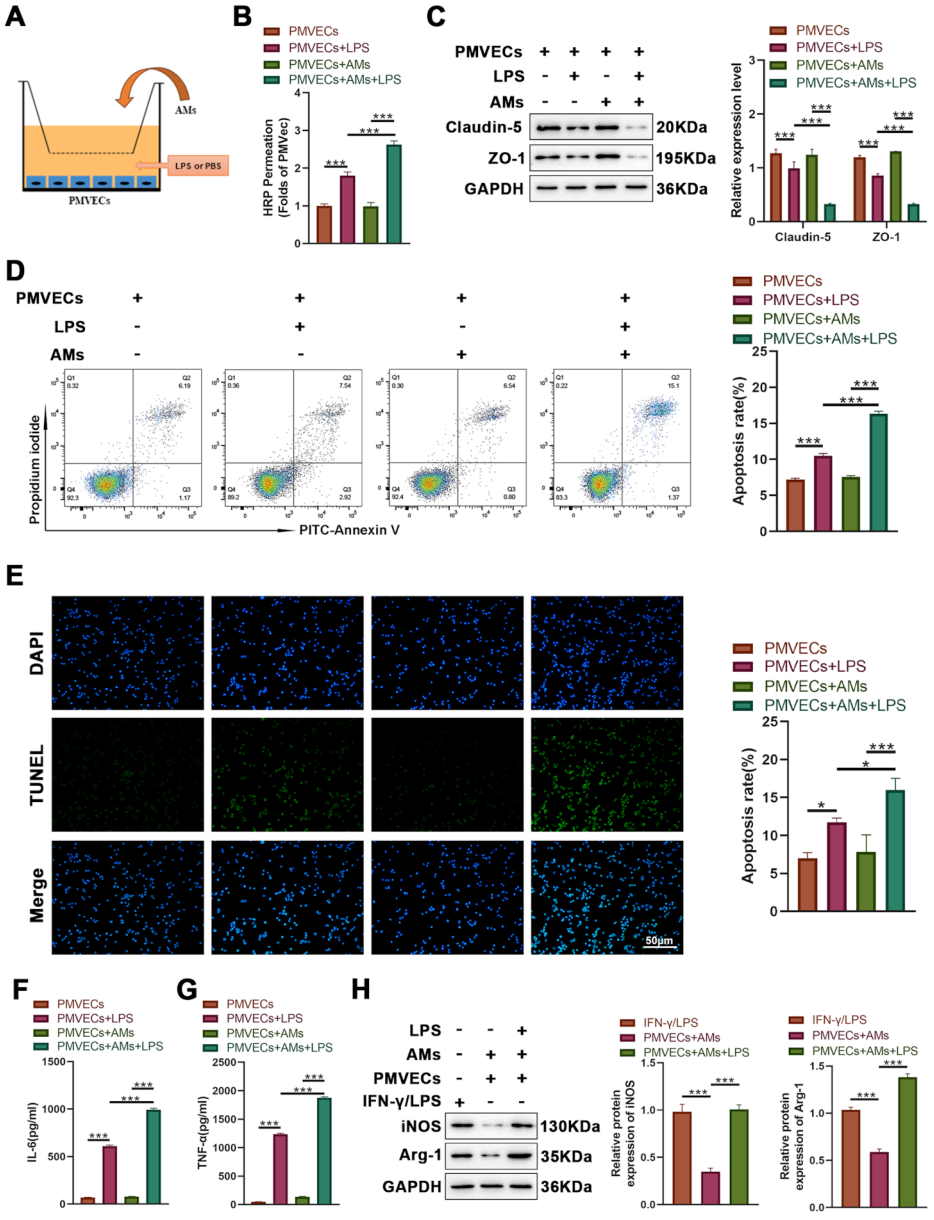

Fig. 1 AMs aggravate LPS-induced injury in PMVECs via M1 polarization-mediated inflammatory response. **(A)** PMVECs were cultured in the presence of AMs or alone, followed by 100 ng/mL LPS treatment. Equivalent PBS was used as the control. After 24 h of culture, **(B)** PMVEC permeability was assessed using HRP leakage assays. **(C)** Western blot analysis revealed the relative expressions of both Claudin-5 and ZO-1 proteins, with GAPDH as the internal reference. **(D)** Annexin V-FITC/PI staining and (E) TUNEL assays demonstrated the apoptosis rate of PMVECs. **(E)** ELISA was used for inflammatory cytokines **(F)** IL-6 and **(G)** TNF-α concentration determination. **(H)** The western blot analysis for iNOS and Arg-1 represented the level of M1 polarization. Data are presented as mean ± SEM. Statistical significance was determined using appropriate methods, with $*p < 0.05$, $***p < 0.001$. PMVECs: pulmonary microvascular endothelial cells; AMs: alveolar macrophages; HRP: horseradish peroxidase

This suggested the enhanced ITA secretion of MSC-exos was probably associated with their protective effects.

ITA mediates the protective effect of MSC-exos on AMs

To investigate whether ITA mediates the protective benefits of MSC-exos on AMs, IRG1 was knocked down in MH-S cells using siRNAs. The knockdown efficiency was validated by PCR and Western blot (Fig. 3A), with the most efficient one selected for further assays. In the co-culture system with si-NC transfected cells, MSC-exos significantly reduced LPS-induced HRP leakage in PMVECs. However, this reduction was not observed in the co-culture system with IRG1 knockdown cells (Fig. 3B). Western blot analysis revealed that MSC-exos significantly increased the expression of Claudin-5 and ZO-1 in PMVECs that co-culture with si-NC transfected

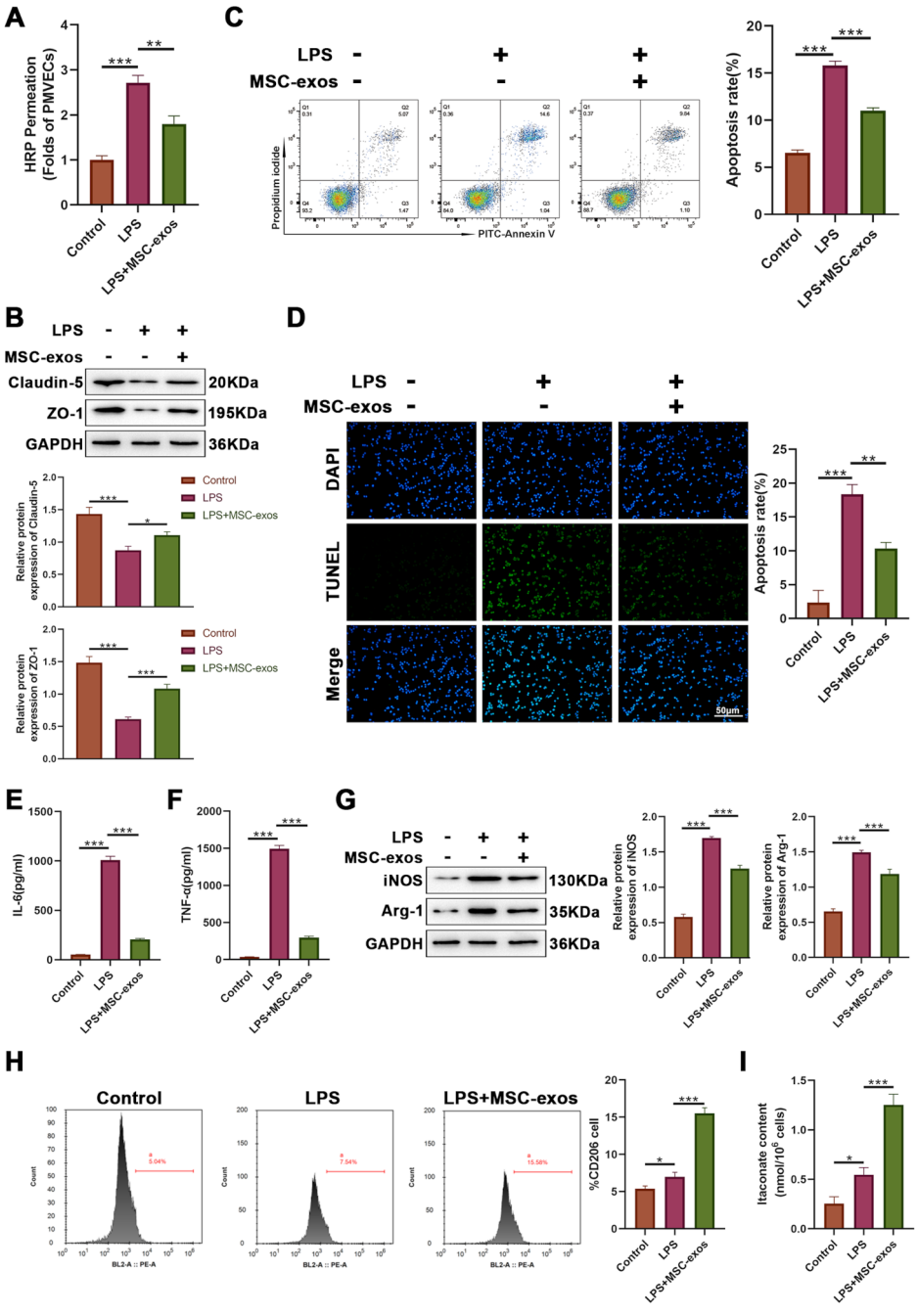

Fig. 2 MSC-exos attenuate LPS-induced PMVEC injury by promoting M2 polarization of AMs. MSC-exos were added to the LPS-treated co-culture system to evaluate their effects on PMVECs. **(A)** PMVEC permeability was assessed using HRP leakage assays. **(B)** Western blot analysis was performed to detect the expression levels of tight junction proteins Claudin-5 and ZO-1. **(C)** Annexin V-FITC/PI staining and **(D)** TUNEL assays demonstrated the apoptosis rate of PMVECs to determine the anti-apoptosis effect of MSC-exos. **(E-F)** ELISA for inflammatory cytokines IL-6 and TNF-α in cell supernatant. **(G)** Western blot analysis for M1 polarization markers assessed the relative levels of iNOS and Arg-1 proteins. **(H)** M2 polarization was determined via flow cytometry by calculate the percentage of CD206-positive cells. **(I)** Gas chromatography-mass spectrometry was used to measure ITA concentration. Data are presented as mean ± SEM. Statistical significance was determined using appropriate methods, with $*p < 0.05$, $**p < 0.01$, and $***p < 0.001$. MSC-exos: mesenchymal stem cell-derived exosome; PMVECs: pulmonary microvascular endothelial cells; AMs: alveolar macrophages; HRP: horseradish peroxidase

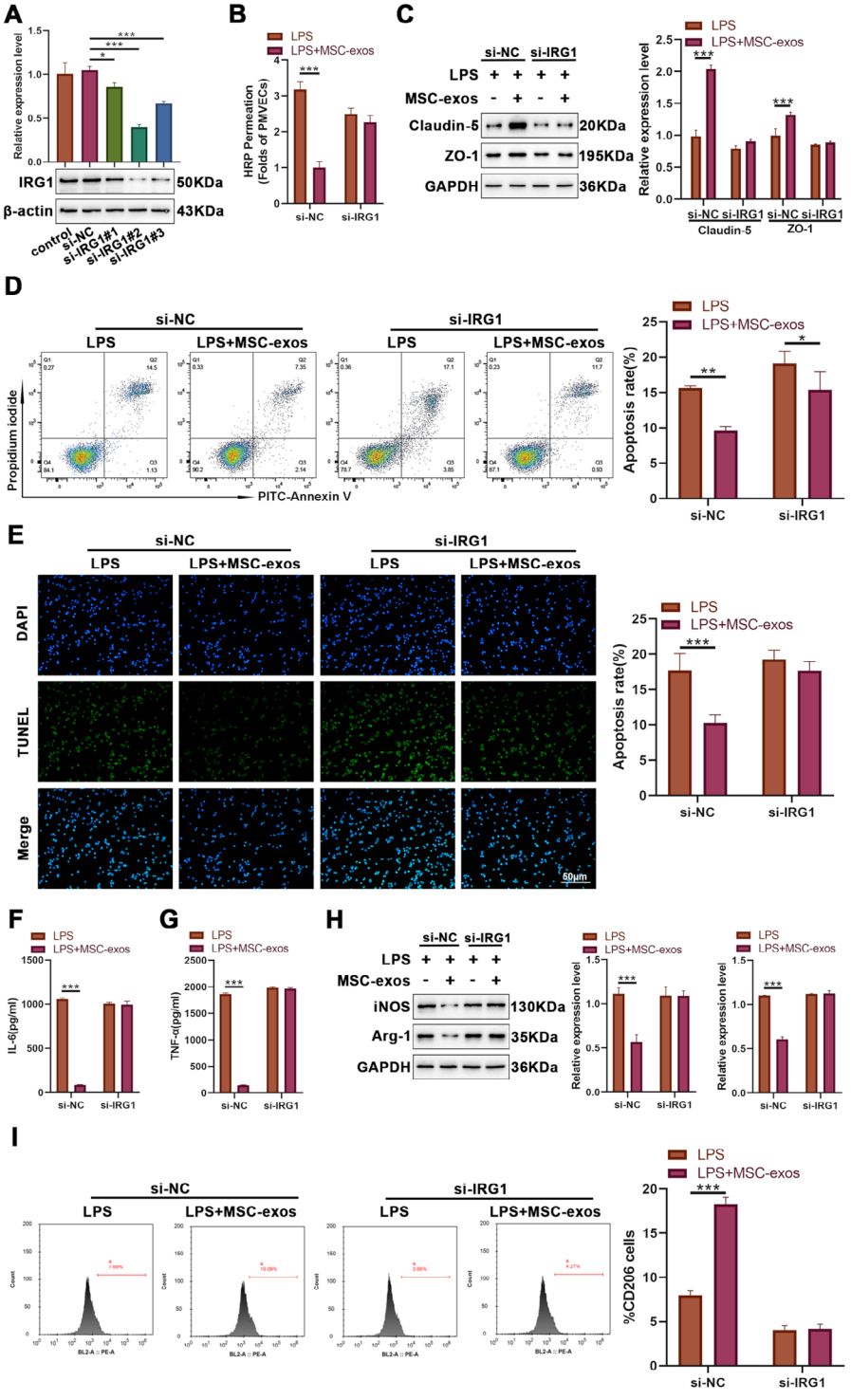

Fig. 3 ITA mediates the effect of MSC-exos on AMs. To investigate the role of ITA, IRG1 was knocked down in MH-S cells using three siRNA-IRG1 with different sequences. si-RNAs were subsequently transfected to the AMs. **(A)** The knockdown efficiency was validated by PCR and Western blot analysis, with the most efficient siRNA selected for further assays. After that, **(B)** the horseradish peroxidase (HRP) permeation assay was conducted and **(C)** western blot analysis revealed the relative levels of tight junction proteins Claudin-5 and ZO-1. Apoptosis rates were assessed using **(D)** Annexin V-FITC/PI staining and **(E)** TUNEL assays. **(F)** ELISA was performed for **(F)** IL-6 and **(G)** TNF-α concentrations. **(H)** For M1 polarization evaluation, iNOS and Arg-1 proteins were determined by Western blot analysis. **(I)** For M2 polarization assessment, the proportion of CD206-positive cells were calculated by flow cytometry. Data are presented as mean ± SEM. Statistical significance was determined using appropriate methods, with *$p < 0.05$, **$p < 0.01$, and ***$p < 0.001$. ITA: itaconic acid; MSC-exos: mesenchymal stem cell-derived exosome; AMs: alveolar macrophages; HRP: horseradish peroxidase

MH-S cells, while no significant change was observed in that co-culture with IRG1 knockdown MH-S cells (Fig. 3C). Annexin V-FITC/PI staining (Fig. 3D) and TUNEL assays (Fig. 3E) were used to assess apoptosis rates. As results, MSC-exos treatment significantly reduced apoptosis of PMVECs in the co-culture system with si-NC transfected cells, but this effect was absent in that with IRG1 knockdown cells (Fig. 3D and E). ELISA assays for inflammatory cytokines IL-6 and TNF-α showed that although MSC-exos significantly decreased the concentration of these cytokines in the co-culture system of si-NC transfected MH-S cells with PMVECs, no significant effect was observed in the co-culture system after knocking down IRG1 in MH-S cells (Fig. 3F and G). For M1 polarization evaluation, iNOS and Arg-1 demonstrated that MSC-exos significantly reduced their expression in si-NC transfected MH-S cells, whereas IRG1 knockdown abolished this effect (Fig. 3H). For M2 polarization assessment, MSC-exos significantly increased the proportion of CD206-positive cells in si-NC transfected MH-S cells, which was inhibited by IRG1 knockdown (Fig. 3I). These findings illustrate the significance of ITA secretion of AMs in the therapeutic potential of MSC-exos.

MSC-exos attenuate LPS-induced acute lung injury in mice by enhancing itaconic acid secretion

C57BL/6 WT and Irg1−/− mice were used to investigate the involvement of ITA in MSC-exos' function in vivo. After the treatment of MSC-exos, the WT mice demonstrated alleviated alveolar structure disruption and inflammatory cell infiltration in lung tissues compared to the group without MSC-exos. Similarly, Irg1−/− mice showed more severe lung tissue damage and extensive inflammation in the LPS group. Although MSC-exos treatment provided relief to a certain extent, significant structural damage and inflammation persisted (Fig. 4A). Additionally, a significantly higher ITA levels in the LPS+MSC-exos group was observed compared to the LPS group in WT mice, while it was almost undetectable in Irg1−/− mice, regardless of MSC-exos treatment (Fig. 4B). In WT mice, lung injury scores were lower with the treatment of MSC-exos compared to the LPS group. But with Irg1 knockdown, no significant difference in lung injury scores was observed between the LPS and LPS+MSC-exos groups (Fig. 4C). The lung wet/dry weight ratio demonstrated that the pulmonary edema was significantly reduced by MSC-exos in WT mice, almost returning to levels similar to the Sham group. Although MSC-exos treatment also reduced the LPS-induced high wet-to-dry weight ratio in Irg1−/− mice, the reduction was limited, with its level remained relatively higher than the Sham control (Fig. 4D). Apart from injury in lung tissues, total protein levels (Fig. 4E) and neutrophils (Fig. 4F) in BALF were significantly suppressed in the LPS+MSC-exos group compared to the LPS group in WT mice. In contrast, this reduction was neglected in Irg1−/− mice. These results demonstrate that ITA secretion was crucial to mediating MSC-exos conferred alleviation in LPS-induced respiratory system injury.

MSC-exos suppress LPS-induced inflammation in ALI mice by regulating the M2 polarization of AMs

To evaluate the anti-inflammatory effects of MSC-exos and the underlying regulatory role of ITA, inflammatory cytokines were initially assessed. MSC-exos treatment significantly reduced the elevated levels of IL-6 and TNF-α induced by LPS in BALF in WT mice, but between the LPS and LPS+MSC-exos groups in Irg1−/− mice there were neglected difference (Fig. 5A and B). Western blot analysis was conducted to assess the M1 polarization, in which both iNOS and Arg-1 were significantly suppressed by MSC-exos in WT mice. However, the MSC-exos treatment failed to reduce the expression of iNOS compared to the LPS group in Irg1−/− mice (Fig. 5C). The M2 polarization was determined via flow cytometry analysis, in which the enhanced proportion of CD206-positive cells elicited by LPS treatment was further enhanced by MSC-exos in WT mice. Notably, in Irg1−/− mice, no significant alteration was found in each group, suggesting that MSC-exos-mediated promotion of M2 polarization is impaired in the absence of ITA (Fig. 5D).

Discussion

ALI is a severe condition with poor prognosis, and understanding its complex regulatory mechanisms is crucial for improving patient outcomes [1]. Our present study elucidates the role of MSC-exos in LPS-induced ALI. Through both co-cultured cells and murine models, we emphasize the critical role of ITA in mediating the protective effects of MSC-exos.

LPS interacts with specific receptors on host cells, leading to the release of various inflammatory mediators to induce oxidative stress and a robust inflammatory response in lung tissue [17]. These properties make LPS a widely used agent in ALI to mimic infection-induced lung damage observed in clinical settings [18, 19]. Consistent with previous studies, our current research demonstrated that LPS disrupts the tight junctions of PMVECs, increases vascular permeability, and results in the leakage of fluids and proteins into the alveolar space, causing pulmonary edema [20, 21]. Notably, AMs play an indispensable role in the process of LPS-mediated PMVEC damage. As the primary immune cells in the lungs, AMs are among the first to encounter inhaled pathogens and toxins, including LPS. They express Toll-like receptor 4,

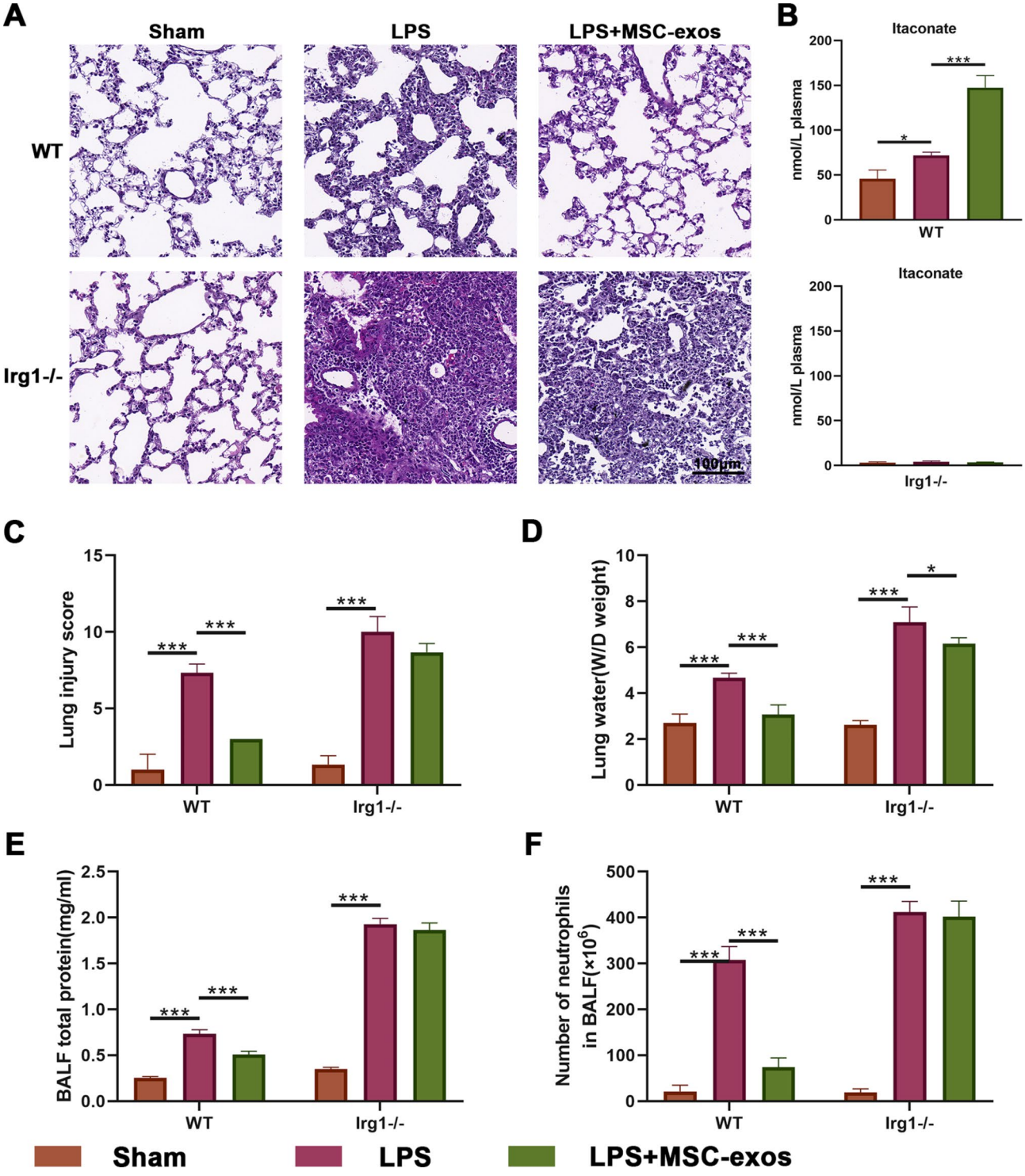

Fig. 4 MSC-exos attenuate LPS-induced acute lung injury in mice by enhancing ITA secretion. C57BL/6 wild-type and IRG1 knockout (Irg1−/−) mice were used to investigate the protective effects of MSC-exos in vivo. After mice were treated with MSC-exos, **(A)** lung tissues were collected and received H&E staining. **(B)** Additionally, ITA concentrations were observed in plasma. **(C)** lung injury scores were calculated according to alveolar edema, hemorrhage, alveolar septal thickening and polymorphonuclear leukocyte infiltration. **(D)** The wet-to-dry weight ratio of the lungs indicated the severity of pulmonary edema. Bronchoalveolar lavage fluid were collected to determine **(E)** total protein levels and **(F)** neutrophil counts. Data are presented as mean ± SEM, with $*p < 0.05$, $***p < 0.001$. ITA: itaconic acid; MSC-exos: mesenchymal stem cell-derived exosome

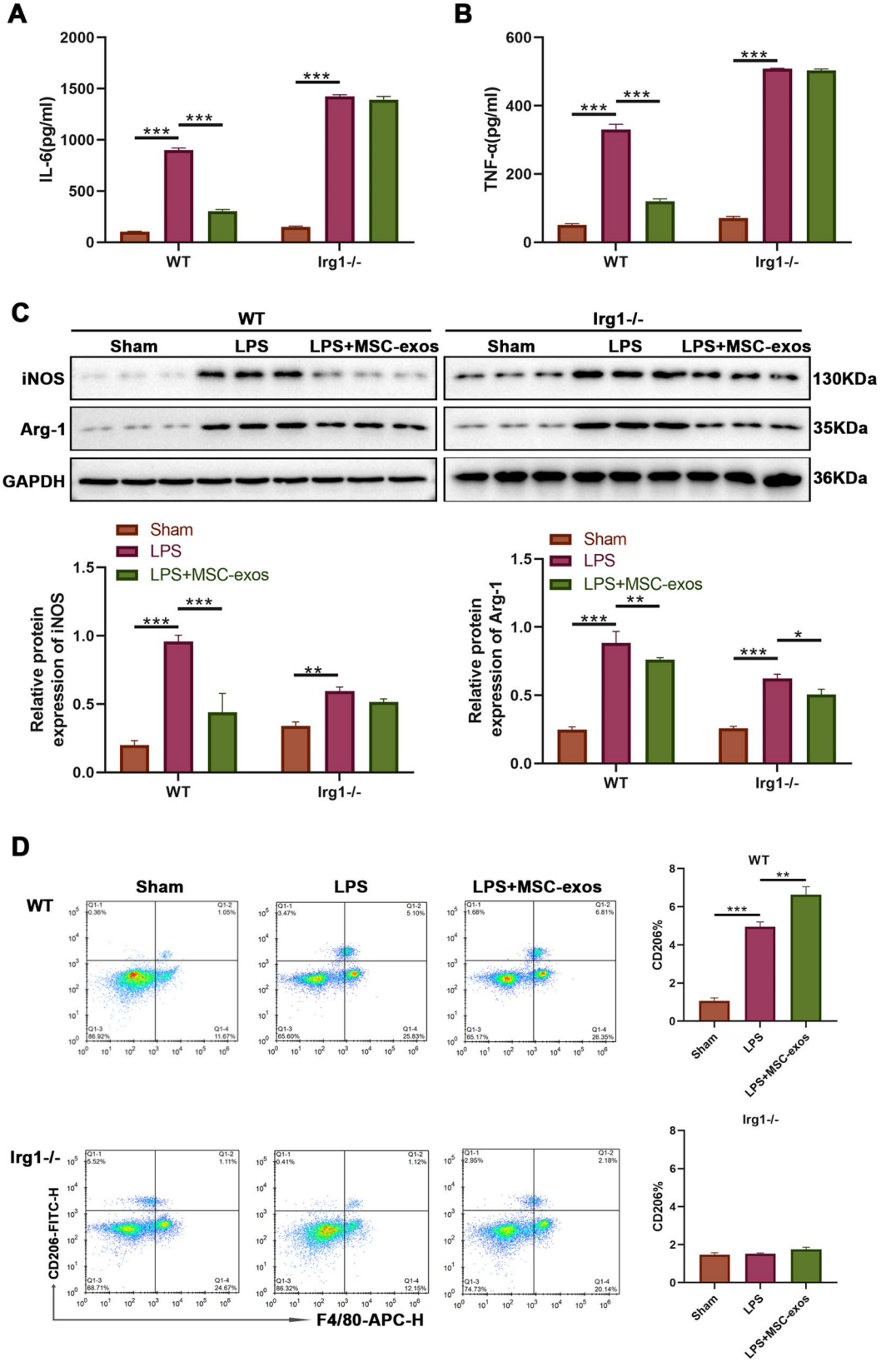

Fig. 5 MSC-exos suppress LPS-induced inflammation in acute lung injury mice by regulating alveolar macrophage polarization. After treatment of MSC-exos, the levels of **(A)** IL-6 and **(B)** TNF-α were assessed in bronchoalveolar lavage fluid of wild-type and Irg1−/− mice. **(C)** iNOS and Arg-1 protein levels were detected by the western blot analysis to assess M1 polarization. **(D)** M2 polarization was determined based on CD206-positive cells via flow cytometry analysis. Data are presented as mean ± SEM. *$p < 0.05$, **$p < 0.01$, and ***$p < 0.001$. MSC-exos: mesenchymal stem cell-derived exosome

which is the key receptor for LPS recognition [22]. In our study, the presence of AMs significantly exacerbated the LPS-induced inflammatory processes. This is consistent with previous research suggesting that the activation and polarization of AMs towards the M1 pro-inflammatory phenotype are of critical significance for the inflammatory storm triggered by LPS [23]. Excessive release of inflammatory cytokines by persistent M1 macrophage activation leads to structural alterations or apoptosis in endothelial cells, ultimately increasing vascular permeability, which is believed to contribute the most to the pathogenesis of ALI [24, 25]. Therefore, strategies to promote M2 macrophage polarization are emerging as potential approaches for the treatment of ALI [26, 27].

The subsequent administration of MSC-exos successfully reversed the damage deteriorated by AMs under LPS stimulation. MSC-exos not only effectively inhibited the permeability and apoptosis of PMVECs but also significantly attenuated the LPS-induced inflammation. This aligns with previous studies showing that MSC-exos have anti-inflammatory and anti-apoptotic effects, protecting various cell types from apoptosis in inflammatory conditions [8]. Meanwhile, our study demonstrated that MSC-exos could enhance the M2 polarization of AMs. ITA-promoting macrophage M2 polarization was confirmed in 2022 [28], of which anti-inflammatory functions in vitro and in vivo through the mechanisms that have been proposed in several investigations [29–31]. A previous study reported that the anti-inflammatory effect of MSC-exos on allergic asthma is attributed to the expanding IL-10 production by lung interstitial macrophages [32]. In the present study, increased ITA levels were observed after the administration of MSC-exos; so we wonder whether the increased production of ITA mediated the protection of MSC-exos on ALI. To deeply investigate the significance of ITA in lung epithelial cells and AMs, we inhibited ITA production by knocking down IRG1 in AMs. IRG1 gene expression is known to be significantly upregulated in macrophages upon pathogen or inflammatory stimulation, leading to increased activity of cis-aconitate decarboxylase and the production of ITA, which demonstrated antimicrobial and anti-inflammatory properties in various diseases [33, 34]. Similarly, when IRG1 was knockdown in AMs, the protective effects of MSC-exos observed in control si-NC AMs were lost and ITA production was inhibited. Specifically, MSC-exos failed to enhance tight junctions, control permeability, and regulate the polarization of macrophages into anti-inflammatory phenotype in the absence of ITA. Notably, despite the inhibition of ITA production following IRG1 knockdown, MSC-exos still exhibited a degree of anti-apoptotic effect on PMVECs, as shown by Annexin V-FITC/PI staining. It primarily detects the phosphatidylserine externalization on the cell surface during early and late apoptosis, whereas TUNEL staining marks DNA fragmentation in late apoptosis [35, 36]. Therefore, while the absence of ITA blocked the inhibition of late apoptosis by MSC-exos, they may still confer protection during slightly earlier stages through alternative mechanisms not solely dependent on ITA production. This might be explained by the direct effect of MSC-exos on vascular endothelial cells. A previous study demonstrated that MSC-exos effectively attenuates thrombin-induced injury on lung microvascular endothelial cells' permeability and junctional integrity [37]. Besides, exosomes from adipose tissue-derived MSCs have been proven to exert endothelial protection via activation of the PI3K/Akt pathway on a histone-induced damage model [38]. Since the present study mainly focused on the mechanism underlying the regulation of MSC-exos on AMs during ALI therapy; whether and how MSC-exos directly protects the endothelium of the ALI model needs to be explored in future studies.

The animal experimental results were consistent with these findings. During ALI, MSC-exos treatment effectively mitigated LPS-induced immune cell activation, inflammatory response stimulation, and disruption of lung epithelial tight junctions. This intervention consequently prevented extensive lung tissue damage and pulmonary edema to some extent. The significant reduction in total protein and neutrophil counts in BALF further underscored the protective effect of MSC-exos on endothelial barrier integrity, inhibiting the infiltration of plasma proteins and immune cells into the alveolar space. These findings are in conformity with previous studies, confirming the protective and inflammation-modulating actions of MSC-exos in ALI mouse models [39, 40]. Notably, the observed protective effects were also accompanied by increased ITA. ITA reduces the production of inflammation-inducing factors and ROS by inhibiting tricarboxylic acid cycle [41]. Our findings highlighted that this metabolic reprogramming of macrophages is crucial for their transition from a pro-inflammatory M1 phenotype to an anti-inflammatory M2 phenotype, which was facilitated at least in part by ITA-induced MSC-exos' function. The resultant M2 macrophages exhibit reduced production of local inflammatory cytokines and promote tissue repair. However, in Irg1−/− mice, where ITA levels were nearly undetectable, the beneficial effects of MSC-exos were abolished. The direct comparison between WT and Irg1−/− mice highlighted ITA as an indispensable mediator of the protective functions of MSC-exos. Taken together, our study, for the first time, uncovered the significant role of ITA in the protective functions of MSC-exos under ALI conditions. Our findings may present a foundation for the protective nature and underlying mechanism of the MSC-exos in ALI and support its promising prospects in cell-free therapies for ALI.

However, there are some limitations in the present study. The potential mechanism underlying the increased ITA levels by MSC-exos remains unclear. Several recent studies demonstrated that MSC-exos can modulate various types of cells by delivering miRNAs or proteins to alleviate ALI [42, 43]. Hence, further analyses such as mass spectrometry and RNA sequence, are required to find the critical components of MSC-exos that induce ITA production. The pathogenesis of ALI is complex, with various cells involved in the development of the disease. This study only focused on the role of MSC-exos in the regulation of AMs during ALI treatment; the direct effect of MSC-exos and the underlying mechanism on other types of cells in ALI need to be explored in future studies.

Conclusions

ITA secretion mediated the protective efficacy of MSC-exos against LPS-induced PMVECs inflammation and apoptosis, as well as ALI in mice by enhancing M2 polarization of AMs. Targeting ITA and regulating macrophage metabolism might be a viable option in the management of ALI and other related inflammatory diseases.

Abbreviations

ALI	Acute lung injury
Ams	Alveolar macrophages
BALF	Bronchoalveolar lavage fluid
DMEM	Dulbecco's Modified Eagle Medium
FBS	Fetal bovine serum
GC	MS-Gas chromatography-mass spectrometry
H&E	Hematoxylin and eosin
ITA	Itaconic acid
LPS	Lipopolysaccharide
MSC	exos-Mesenchymal stem cell-derived exosomes
NTA	Nanoparticle tracking analysis
PCR	Polymerase chain reaction
PMVECs	Pulmonary microvascular endothelial cells
p/s	penicillin/streptomycin-glutamine
TEM	Transmission electron microscopy
WT	Wild-type
ZO	1-Zonula occludens-1

Supplementary Information

The online version contains supplementary material available at https://doi.org/10.1186/s13062-024-00586-8.

Supplementary Material 1

Supplementary Material 2

Supplementary Material 3

Supplementary Material 4

Acknowledgements

None.

Author contributions

YMW and ZAL designed experiments, carried out experiments, analyzed experimental results. YMW wrote the manuscript. ZAL revised the manuscript. All authors approved the final manuscript.

Funding

This research did not receive any specific grant from funding agencies in the public, commercial, or not-for-profit sectors.

Data availability

The data that support the findings of this study are available from the corresponding author upon reasonable request.

Declarations

Ethics approval and consent to participate

All animal experiments were conducted aligned with the guidelines of Institutional Animal Care and Use Committee. Prior to the initiation of the study, approval was obtained from the ethics commitee of Sichuan University.

Consent for publication

Not applicable.

Competing interests

The authors declare no competing interests.

Received: 12 August 2024 / Accepted: 11 December 2024
Published online: 26 December 2024

References

1. Mowery NT, Terzian WH, Nelson AC. Acute lung injury. Curr Probl Surg. 2020;57:100777.
2. Zoulikha M, Xiao Q, Boafo GF, Sallam MA, Chen Z, He W. Pulmonary delivery of siRNA against acute lung injury/acute respiratory distress syndrome. Acta Pharm Sinica B. 2022;12:600–20.
3. Lin X, Barravecchia M, Kothari P, Young J, Dean D, β1-Na+. K+-ATPase gene therapy upregulates tight junctions to rescue lipopolysaccharide-induced acute lung injury. Gene Ther. 2016;23:489–99.
4. Gupta S, Short SA, Sise ME, Prosek JM, Madhavan SM, Soler MJ, et al. Acute kidney injury in patients treated with immune checkpoint inhibitors. J Immunother Cancer. 2021;9:e003467.
5. Nikfarjam S, Rezaie J, Zolbanin NM, Jafari R. Mesenchymal stem cell derived-exosomes: a modern approach in translational medicine. J translational Med. 2020;18:1–21.
6. Zhu J, Zhou J, Feng B, Pan Q, Yang J, Lang G, et al. MSCs alleviate LPS-induced acute lung injury by inhibiting the proinflammatory function of macrophages in mouse lung organoid–macrophage model. Cell Mol Life Sci. 2024;81:124.
7. Xia L, Zhang C, Lv N, Liang Z, Ma T, Cheng H, et al. AdMSC-derived exosomes alleviate acute lung injury via transferring mitochondrial component to improve homeostasis of alveolar macrophages. Theranostics. 2022;12:2928.
8. Arabpour M, Saghazadeh A, Rezaei N. Anti-inflammatory and M2 macrophage polarization-promoting effect of mesenchymal stem cell-derived exosomes. Int Immunopharmacol. 2021;97:107823.
9. Ning L, Shishi Z, Bo W, Huiqing L. Targeting immunometabolism against acute lung injury. Clin Immunol. 2023;249:109289.
10. Sano M, Tanaka T, Ohara H, Aso Y. Itaconic acid derivatives: structure, function, biosynthesis, and perspectives. Appl Microbiol Biotechnol. 2020;104:9041–51.
11. Zhu X, Guo Y, Liu Z, Yang J, Tang H, Wang Y. Itaconic acid exerts anti-inflammatory and antibacterial effects via promoting pentose phosphate pathway to produce ROS. Sci Rep. 2021;11:18173.
12. Lampropoulou V, Sergushichev A, Bambouskova M, Nair S, Vincent EE, Loginicheva E, et al. Itaconate links inhibition of succinate dehydrogenase with macrophage metabolic remodeling and regulation of inflammation. Cell Metabol. 2016;24:158–66.
13. Weiss JM, Palmieri EM, Gonzalez-Cotto M, Bettencourt IA, Megill EL, Snyder NW, et al. Itaconic acid underpins hepatocyte lipid metabolism in non-alcoholic fatty liver disease in male mice. Nat Metabolism. 2023;5:981–95.
14. Maeß MB, Wittig B, Lorkowski S. Highly efficient transfection of human THP-1 macrophages by nucleofection. JoVE (Journal Visualized Experiments). 2014;e51960.
15. Liu L, Stokes JV, Tan W, Pruett SB. An optimized flow cytometry panel for classifying macrophage polarization. J Immunol Methods. 2022;511:113378.
16. Soini Y. Claudins in lung diseases. Respir Res. 2011;12:1–11.

17. Tang J, Xu L, Zeng Y, Gong F. Effect of gut microbiota on LPS-induced acute lung injury by regulating the TLR4/NF-kB signaling pathway. Int Immunopharmacol. 2021;91:107272.
18. Nguyen N, Xu S, Lam TYW, Liao W, Wong WF, Ge R. ISM1 suppresses LPS-induced acute lung injury and post-injury lung fibrosis in mice. Mol Med. 2022;28:72.
19. Ye R, Liu Z. ACE2 exhibits protective effects against LPS-induced acute lung injury in mice by inhibiting the LPS-TLR4 pathway. Exp Mol Pathol. 2020;113:104350.
20. Ren Y, Li L, Wang M-M, Cao L-P, Sun Z-R, Yang Z-Z, et al. Pravastatin attenuates sepsis-induced acute lung injury through decreasing pulmonary microvascular permeability via inhibition of Cav-1/eNOS pathway. Int Immunopharmacol. 2021;100:108077.
21. Wang Y, Wang Y, Ma J, Li Y, Cao L, Zhu T, et al. YuPingFengSan ameliorates LPS-induced acute lung injury and gut barrier dysfunction in mice. J Ethnopharmacol. 2023;312:116452.
22. Wang J, Li R, Peng Z, Hu B, Rao X, Li J. HMGB1 participates in LPS–induced acute lung injury by activating the AIM2 inflammasome in macrophages and inducing polarization of M1 macrophages via TLR2, TLR4, and RAGE/NF–κB signaling pathways Corrigendum in/10.3892/ijmm. 2020.4530. Int J Mol Med. 2020;45:61–80.
23. Wang Z, Wang Z. The role of macrophages polarization in sepsis-induced acute lung injury. Front Immunol. 2023;14:1209438.
24. Lu HL, Huang XY, Luo YF, Tan WP, Chen PF, Guo YB. Activation of M1 macrophages plays a critical role in the initiation of acute lung injury. Biosci Rep. 2018;38:BSR20171555.
25. Maniatis NA, Kotanidou A, Catravas JD, Orfanos SE. Endothelial pathomechanisms in acute lung injury. Vascul Pharmacol. 2008;49:119–33.
26. Liu H, He Y, Lu C, Zhang P, Zhou C, Ni Y, et al. Efficacy of pulmonary transplantation of engineered macrophages secreting IL-4 on acute lung injury in C57BL/6J mice. Cell Death Dis. 2019;10:664.
27. Xia L, Zhang C, Lv N, Liang Z, Ma T, Cheng H, et al. AdMSC-derived exosomes alleviate acute lung injury via transferring mitochondrial component to improve homeostasis of alveolar macrophages. Theranostics. 2022;12:2928–47.
28. Ni L, Lin Z, Hu S, Shi Y, Jiang Z, Zhao J, et al. Itaconate attenuates osteoarthritis by inhibiting STING/NF-κB axis in chondrocytes and promoting M2 polarization in macrophages. Biochem Pharmacol. 2022;198:114935.
29. Lampropoulou V, Sergushichev A, Bambouskova M, Nair S, Vincent EE, Loginicheva E, et al. Itaconate Links Inhibition of Succinate Dehydrogenase with Macrophage Metabolic Remodeling and Regulation of Inflammation. Cell Metab. 2016;24:158–66.
30. Bambouskova M, Gorvel L, Lampropoulou V, Sergushichev A, Loginicheva E, Johnson K, et al. Electrophilic properties of itaconate and derivatives regulate the IκBζ-ATF3 inflammatory axis. Nature. 2018;556:501–4.
31. Mills EL, Ryan DG, Prag HA, Dikovskaya D, Menon D, Zaslona Z, et al. Itaconate is an anti-inflammatory metabolite that activates Nrf2 via alkylation of KEAP1. Nature. 2018;556:113–7.
32. Ren J, Liu Y, Yao Y, Feng L, Zhao X, Li Z, et al. Intranasal delivery of MSC-derived exosomes attenuates allergic asthma via expanding IL-10 producing lung interstitial macrophages in mice. Int Immunopharmacol. 2021;91:107288.
33. Li Y, Zhang P, Wang C, Han C, Meng J, Liu X, et al. Immune responsive gene 1 (IRG1) promotes endotoxin tolerance by increasing A20 expression in macrophages through reactive oxygen species. J Biol Chem. 2013;288:16225–34.
34. Li Y, Gong W, Li W, Liu P, Liu J, Jiang H, et al. The IRG1-Itaconate axis: A regulatory hub for immunity and metabolism in macrophages. Int Rev Immunol. 2023;42:364–78.
35. Kyrylkova K, Kyryachenko S, Leid M, Kioussi C. Detection of apoptosis by TUNEL assay. Odontogenesis: methods and protocols. 2012;41 – 7.
36. Alshehade SA, Almoustafa HA, Alshawsh MA, Chik Z. Flow cytometry-based quantitative analysis of cellular protein expression in apoptosis subpopulations: A protocol. Heliyon. 2024;10:e33665.
37. Potter DR, Miyazawa BY, Gibb SL, Deng X, Togaratti PP, Croze RH, et al. Mesenchymal stem cell-derived extracellular vesicles attenuate pulmonary vascular permeability and lung injury induced by hemorrhagic shock and trauma. J Trauma Acute Care Surg. 2018;84:245–56.
38. Mizuta Y, Akahoshi T, Guo J, Zhang S, Narahara S, Kawano T, et al. Exosomes from adipose tissue-derived mesenchymal stem cells ameliorate histone-induced acute lung injury by activating the PI3K/Akt pathway in endothelial cells. Stem Cell Res Ther. 2020;11:508.
39. Wang C, Jiang C, Yang Y, Xi C, Yin Y, Wu H, et al. Therapeutic potential of HUC-MSC-exos primed with IFN-γ against LPS-induced acute lung injury. Iran J Basic Med Sci. 2024;27:375.
40. Xu B, Chen S-s, Liu M-z, Gan C-x, Li J-q. Guo G-h. Stem cell derived exosomes-based therapy for acute lung injury and acute respiratory distress syndrome: a novel therapeutic strategy. Life Sci. 2020;254:117766.
41. Yang C, Liu T, Shi G-P. Therapeutic potential of tricarboxylic acid cycle metabolite itaconate in cardiovascular diseases. EBioMedicine. 2020;59:102938.
42. Liu P, Yang S, Shao X, Li C, Wang Z, Dai H, et al. Mesenchymal Stem Cells-Derived Exosomes Alleviate Acute Lung Injury by Inhibiting Alveolar Macrophage Pyroptosis. Stem Cells Transl Med. 2024;13:371–86.
43. Lin WT, Wu HH, Lee CW, Chen YF, Huang L, Hui-Chun Ho J, et al. Modulation of experimental acute lung injury by exosomal miR-7704 from mesenchymal stromal cells acts through M2 macrophage polarization. Mol Ther Nucleic Acids. 2024;35:102102.

Publisher's note